Flow, heat conductivity, and gas diffusion in partly saturated microstructures

Volker Schulz, Dirk Kehrwald, Andreas Wiegmann, Konrad Steiner

Fraunhofer-Institut für Techno- und Wirtschaftsmathematik, Kaiserslautern, Germany

Summary:

The calculation of effective material properties of porous media based on the underlying 3D geometry had been established over the last years. In this context, the prediction of the permeability based on the pore geometry only is a very common example.

For many industrial applications such as dewatering of paper, the porous media is partly saturated with significant changes of its properties such as the permeability, the gas diffusion, or the heat conductivity.

Here, we present a new approach to predict these relative material properties based on its 3D pore space only which is a challenge up to now. Our method includes a drainage simulation based on morphological operations and the solution of appropriate PDEs. We demonstrate the capability of our approach for a prediction of relative material parameters of a carbon paper used as a diffusion media in a fuel cell.

Keywords:

Microstructure simulation, capillary pressure-saturation, relative permeability, effective gas diffusion, effective heat transfer, virtual material design, diffusion media, fuel cell

1 Introduction

Two-phase flow phenomena in porous media have wide application, e.g. wetting and drying of sanitary products, paper production or processes in a fuel cell. In this paper, we are using the example of a diffusion media in a fuel cell in order to present a new approach for the determination of relative material properties based on the underlying microstructure.

1.1 Fuel cell and specific functions of the diffusion media

A fuel cell is a device that uses hydrogen and oxygen to create electricity by an electrochemical process. A possible technical realization are polymer electrolyte fuel cells (PEFC) where the two gases combine at a membrane of about 50µm thickness covered with a catalytic layer. The membrane is surrounded by a gas-diffusion media of about 200µm thickness [5]. In this setup the gas-diffusion media plays an important role since it has several specific functions

- Provide a continuous transport of the reactant gases to the membrane even if the medium is partly filled with the product water
- Provide a passage for the removal of water from the membrane to flow-field channels
- Provide an efficient heat removal for a stable operating temperature
- Provide electronic conductivity between anode and cathode

Obviously finding a diffusion media with optimal performance is challenging since the entire list of properties have to be optimized together. In this context, the simulation of material properties can be used to develop an optimization strategy for a selected material. This can be done without the need of manufactured prototypes.

2 Microstructure modeling

The determination of the material properties by computer simulation which are shown in this paper are entirely based on the underlying geometry. Therefore it is mandatory to generate a representative 3D-geometry of the material. In principal there are two possible approaches [3]. The first one includes image giving methods such as synchrotron or X-ray tomography. The second one which is used in this paper is a reconstruction of the geometry based on statistical material parameters such as porosity and mean fiber thicknesses. Beside the fact that a tomography of a sample with a required resolutions down to 1µm is costly, the latter approach allows the virtual modification of material parameter. Additionally, the method works quite good for non-woven structures as shown already in [7] and [8].

2.1 Fiber structures

Following [5] the most promising candidates for use as diffusion media in PEFCs are carbon-fiber-based products, e.g. non-woven papers with porosities of 70% or higher and a good electrical conductivity.

For the work presented in this paper, we generated a 3D-geometry in order to represent the carbon-fiber paper Toray TGP-H-60 with mean fiber diameters of 7µm and a porosity of 80% as specified in [5]. Due to the manufacturing process, the orientation of the carbon fibers is strongly anisotropic so that one can distinguish a through-plane and an in-plane direction. Without going into detail, the fibers are impregnated by a resin for reinforcement which was also included in our reconstruction procedure (see Fig. 1).

But we have to mention that there is too few information about the microstructure given in [5] so that we were not looking forward to a 1:1 reconstruction of the media. As a consequence, we do not expect that our simulation result entirely agree with published data. The objective of this work is only to demonstrate the principles of our approach. Detailed studies in comparison to measured data will follow in later studies.

Due to a coating of the fibers with Teflon (PTFE), the carbon paper is hydrophobic. Therefore, in the following, the gas phase is treated as the wetting phase while water is a non-wetting phase for the media, respectively. Typical contact angles ranging from 115° up to 165° depending on the Teflon amount [5].

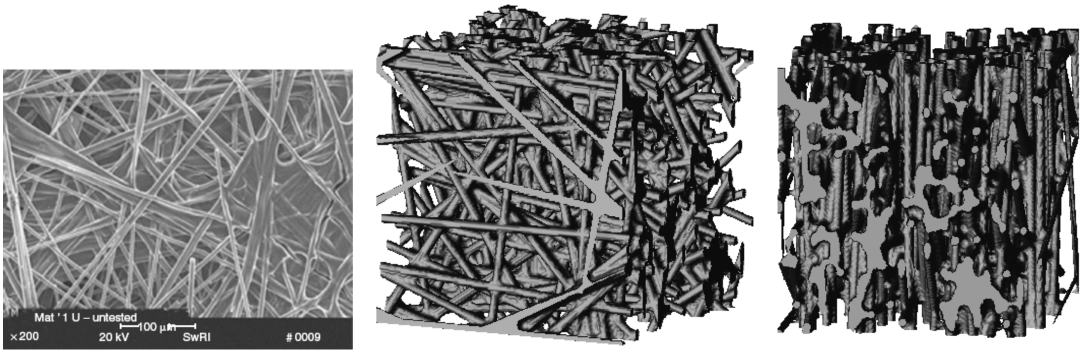

Fig. 1: Micrograph (scanning electron microscope – SEM) of the Toray TGP-H-60 and a visualization of the reconstructed 3D-geometry. On the right hand side one can clearly see the strong anisotropy of the material and the simulated resin between the fibers. The resolution of the reconstruction is 0.7µm which corresponds to a sample size of 180x180x180µm.

3 Simulation of two-phase distributions in a drainage process

An important step for the determination of properties for partly saturated materials is to model the saturation in dependence of the capillary pressure.

3.1 Full-morphology approach (FM)

As shown in [2] and [11], it is possible to simulate the stationary distribution of water and gas for an arbitrary capillary pressure p_c on the basis of a complete three-dimensional structure by a so-called full-morphology (FM) approach. The basic idea behind the FM model is that at a given capillary pressure p_c the pore space accessible for the water[1] is in the first place determined by the size of the pores. Within the complex structure of porous media, the hydraulic size of the pore space at a given location can be defined by the mean curvature radius of the interface between water and air that can be established at this location. The capillary pressure is identified by the principal radii of curvature of this interface, r_1 and r_2,

$$p_c = \sigma \left(\frac{1}{r_1} + \frac{1}{r_2} \right) \cos \alpha \,, \qquad (1)$$

given the surface tension σ between the wetting (gas) and the non-wetting phase (water) and the contact angle α between the wetting and the solid phase. To determine the part of the pore space that will be accessible for the non-wetting phase at a given pressure during drainage, we first decompose the image with the pore radius as ordering parameter. This is done by a morphological opening with spheres of increasing size. This method determines the part of the pore space where the test sphere fits in. Hence, the 'opened' pore space can be associated with the pore volume occupied by the non-wetting phase while the residual pore volume is occupied by the wetting phase. So far, this approach corresponds to the concept of granulometry where details can be found in textbooks, e.g. [10].

Due to the spherical elements used in the morphological operation, we assume that the interfaces between the water and the gas in the porous media can be approximated by spherical caps. Thus, equation (1) is simplified to

$$p_c = \frac{2\sigma}{r} \cos \alpha \,. \qquad (2)$$

For the simulation of a drainage process the morphological operations are completed with appropriate boundary conditions and a test for connectivity of the water.

Thus, the steps of our algorithm to determine the quasi-static primary drainage curve are as follows:

- At the beginning, the complete pore space is air filled, i.e. p_c =0. At one side, the medium is connected to a air phase reservoir while at the opposite side it is connection to a water phase reservoir. The other four sides of the cubic domain are considered to be impermeable for water and gas.
- We start with the maximum possible pore radius $r=r_{max}$ determine the space of all pores with

---

[1] Please note again that the investigated material is hydrophybic and therefore water is the non-wetting phase while air is the wetting phase in the two-phase processes.

  - a radius larger or equal to r and
  - which are connected to the water reservoir
- From the so-determined pore space, we can directly calculate the saturation from the volume fraction of each phase and relate that to a capillary pressure according to the Young-Laplace equation (2).
- This procedure is repeated with stepwise reduced radii until the entire pore space is filled with water, i.e. the non-wetting fluid.

We refer to [2], [9], and [11] for details of the implementation since one has to be careful when applying morphological operations on voxel images.

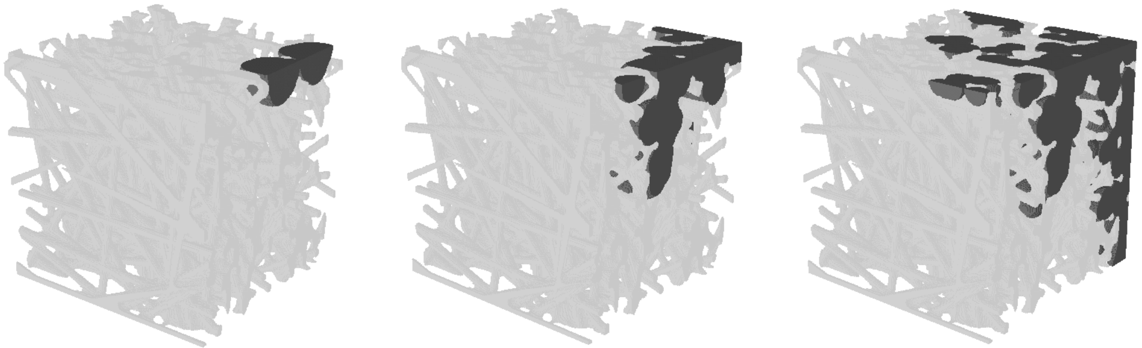

Fig. 2: Water penetrates from the top of the sample into the accessible pore space. The capillary decreases from the left to the right hand side due to an increase of the water saturation.

The application of the full-morphology method on the carbon paper is illustrated for 3 different saturations corresponding to different capillary pressures in Fig. 2.

4 Absolute and relative material properties

4.1 Absolute permeability

We define **absolute** material properties of microstructures as a mean property of the material when the entire pore space is filled with a fluid of one type only. The determination of the absolute (or intrinsic) permeability of a material based on the 3D microstructure was discussed by [3] already and will be summarized shortly in the following.

For convenience, we assume that the edges of the sample are parallel to the cartesian coordinate axes. The mathematical basis of this procedure is Darcy's law for flow in porous media,

$$\bar{\boldsymbol{u}} = -\frac{1}{\mu}\mathsf{K}\,\mathrm{grad}\,p, \qquad (3)$$

where $\bar{\boldsymbol{u}}$ denotes the average flow velocity and K represents the permeability tensor of the porous medium. The component k_{ij} of the permeability tensor represents the permeability of the material in the direction parallel to the jth coordinate axis if the main flow direction is parallel to the ith coordinate axis. As a direct consequence, the off-diagonal elements of K are equal to zero. Furthermore, if the pressure gradient and, therefore, the main flow direction are parallel to the ith coordinate axis, Darcy's law reduces to the scalar equation

$\bar{u}_i = -\frac{k_{ii}}{\mu L}\delta p,$ which can be rewritten in the form $k_{ii} = -\frac{\mu L \bar{u}_i}{\delta p}.$

Above, $\bar{u}_i$ is the average flow speed, L represents the length of that edge of the sample which is parallel to the ith coordinate axis, and δp stands for the pressure drop parallel to the ith coordinate axis. The present situation is visualised in Fig. 3.

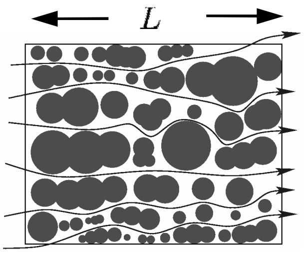

Fig. 3: A 2d porous medium, main flow direction from left to right, the edges parallel to the main flow direction have length L

Now, we choose appropriate values for μ as well as δp and determine $\bar{u}_i$ for $i=1,2,3$ by solving the Stokes equations using a Lattice Boltzmann method.

4.1.1 Lattice Boltzmann methods

For an overview of the lattice Boltzmann method, we refer to [4] and give only a short overview in the following. Lattice Boltzmann methods are special numerical schemes for solving the incompressible Navier-Stokes equations,

$$\operatorname{div} \boldsymbol{u} = 0 \quad \text{and} \quad \partial_t(\rho \boldsymbol{u}) + \operatorname{div}(\rho \boldsymbol{u} \otimes \boldsymbol{u}) = -\nabla p + \mu \Delta \boldsymbol{u}, \qquad (4)$$

where $\boldsymbol{u}$ stands for the fluid velocity, ρ represents density, p denotes pressure, μ represents viscosity, and $\otimes$ stands for the tensor product of two vectors.

In lattice Boltzmann methods, instead of discretizing the Navier-Stokes equations directly we simulate particle dynamics on a mesoscopic scale. For this purpose we discretize the computational domain using a regular lattice with equidistant nodes. At each time t, we consider the particle density $f(t,\boldsymbol{x};\boldsymbol{v})$ located lattice node $\boldsymbol{x}$ and moving with lattice velocity $\boldsymbol{v}$, where $\boldsymbol{v}$ can only take certain constant values that make sure the particle density is moving from one lattice point to another during one time step.
The lattice Boltzmann equation takes the form [6]

$$f(t+\delta t, \boldsymbol{x}+\boldsymbol{v}\delta t;\boldsymbol{v}) = f(t,\boldsymbol{x};\boldsymbol{v}) + \mathrm{Q}(f)(t,\boldsymbol{x};\boldsymbol{v}),$$

where Q represents the so-called collision operator. There are several possibilities to choose the collision operator, each of them defining a special lattice Boltzmann scheme. The macroscopic quantities p and $\boldsymbol{u}$ are obtained via averaging,

$$p(t,\boldsymbol{x}) = c_s^2 \sum_{\boldsymbol{v}} f(t,\boldsymbol{x};\boldsymbol{v}) \quad \text{and} \quad \boldsymbol{u}(t,\boldsymbol{x}) = \frac{\sum_{\boldsymbol{v}} \boldsymbol{v} f(t,\boldsymbol{x};\boldsymbol{v})}{\sum_{\boldsymbol{v}} f(t,\boldsymbol{x};\boldsymbol{v})}$$

with a lattice dependent constant c_s^2. The tuple $(p,\boldsymbol{u})$ is then an approximation of first order in time of the macroscopic Navier-Stokes equations.

4.2 Relative permeability

The relative permeability K_S is defined by an extension of the Darcy's law to

$$\bar{\mathbf{u}} = -\frac{1}{\mu} \mathrm{K_S}(\,\mathrm{S})\ \mathrm{grad}\, p, \qquad (4)$$

also known as Buckingham-Darcy's law where the index 'S' reflects that the permeability depends on the saturation media. Obviously, using equation (4) we can define a relative permeability for the both, the wetting and the non-wetting fluid. The calculation of the relative permeabilities for a given phase distribution is difficult and requires solving the Navier-Stokes equation for each phase with appropriate boundary conditions at the interface of the phases.

Here we propose a new method which is based on the assumption that the relative permeability of the phases can be decoupled which is valid as long as the capillary forces are large compared to the viscous forces. In other words, the streaming of one phase does not change the configurations of the phases. This is a valid assumption when using the phase distribution as calculated in the full-morphology model especially for small values of the water saturation. Fig. 4 illustrates how under these assumptions the relative gas permeability can be calculated from the reduced accessible pore space.

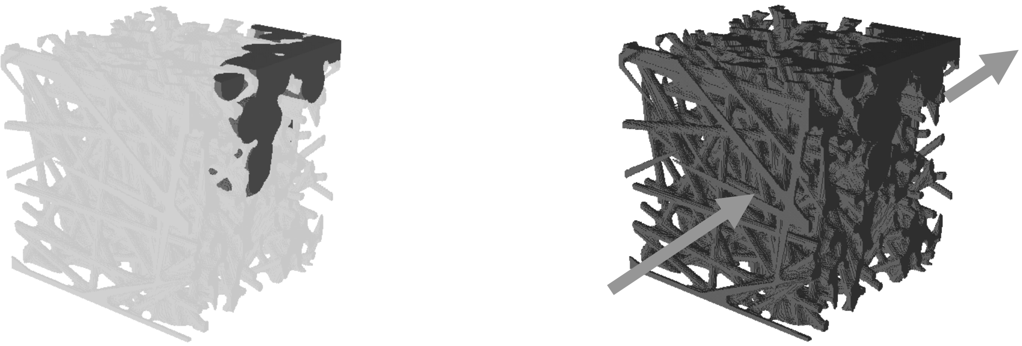

Fig. 4: The relative permeability of the gas phase is estimated by calculating the flow field in the pore space occupied by the gas. An interaction between water and gas phase is neglected. The arrows on the right hand side indicate the streaming direction which is perpendicular to the boundary conditions of the simulated drainage process.

Therefore, we have decomposed the complicated two-phase problem into the streaming of the single phases independently from each other. To solve the Stokes problem for a given saturation (as determined by the drainage simulation) we use the same lattice Boltzmann method as described above.

4.3 Heat conductivity

In analogy to the absolute permeability one defines the effective heat conductivity tensor β_{eff} for a material by using Fouries law:

$$j = -\beta_{eff}\, \mathrm{grad}\, T\,, \qquad (5)$$

where *j* is the heat flux and *T* the temperature. If the heat transfer is based only on heat diffusion the determination of β_{eff} leads to the following heat equation on the microscopic level

$$\mathrm{grad} \cdot (\beta \cdot \mathrm{grad}\, u) = f\,, \qquad (6)$$

where *u* is the local temperature, β the local heat conductivity and *f* a heat source.

Now, β_{eff} can be found by the following procedure: At first we determine the temperature distribution in the material by solving equation (6) with appropriate boundary conditions. For practically relevant problems, a numerical solution is usually necessary. If the oscillations of the β are periodic then it is possible to apply homogenization theory. This allows to find a constant tensor β_{eff} which can be used for finding the mean temperature field, without local fluctuations due to inhomogeneities. Following the homogenization theory for estimation of β_{eff} in the 3D case it is necessary to solve 3 different periodic problems (l=1,2,3) in the unit cell Ω=(0,1)x(0,1)x(0,1):

$$
\begin{aligned}
&-\mathrm{grad}(\beta(\vec{x})(\mathrm{grad}\, U_l+\vec{e}_l))=0,\ \ x\in\Omega \\
&U_l(\vec{x}+\vec{e}_m)=U_i(\vec{x}),\ m=1,2,3
\end{aligned}
\qquad (7)
$$

Where e_l is the unit vector in the direction x_l. One finds three solution U_1, U_2, U_3. The components of the averaged conductivity tensor can be estimated by integration:

$$\beta_{lm}^{eff}=\int \beta(\vec{x})(gradU_l+\vec{e}_l)\vec{e}_m dx,\ \ l=1,2,3;\ m=1,2,3$$

For technical details of solving equation (7) we refer to [12]. Let us mention that the solver has to deal with large jumps in β due to large differences of the local heat conductivity. Note that for example the (diffusive) heat conductivity between air and a solid differs in general by orders of magnitude.

4.4 Absolute gas diffusion

The determination of the absolute gas diffusion coefficient of a material follows exactly the approach used for the heat conductivity. This is due to the fact that Fick's first law

$$j=-D_{eff}\,\mathrm{grad\ c}, \qquad (8)$$

which describes the diffusion process has the same structure as Fouries law of heat transfer. In equation (7) j denotes the average concentration flux velocity. D_{eff} represents the tensor of effective gas diffusion. For convenience, we define D_{eff} as the unity tensor for diffusion in free space without any medium. Thus, we do not have to correct the results by the (physical) diffusion constant of the gas. As a benefit of that definition, we can directly calculate the tortuosity τ of the material as

$$\tau=\sqrt{\frac{\phi}{D_{eff}}}, \qquad (9)$$

where ϕ is the porosity of the media [1]
In contrast to the heat flux, the gas diffusion is zero within the solid which corresponds to β=0 or no-flux boundary conditions on the surface:

$$\vec{\mathrm{n}}\cdot\mathrm{grad}\, c=0\,. \qquad (10)$$

Beside that, the calculation of the effective gas diffusion coefficient follows the same averaging procedure as for the heat conductivity.

4.5 Relative gas diffusion

When the media is partly saturated with a liquid phase the effective gas diffusion coefficient becomes saturation dependent.
Based on two assumption, we can use the same approach as for the relative permeability in order to calculate the relative gas diffusion coefficient.

- The diffusion from the gas phase into the liquid phase can be neglected.
- Thus, the transport of the gas within the liquid phase (as dissolved gas) is also negligible.

These two assumptions correspond to no-flux boundary conditions between gas and liquid phase. Thus the relative gas diffusion can be calculated for successive saturations based on the gas/liquid phase distributions coming from the simulated drainage process as illustrated in Fig. 5.

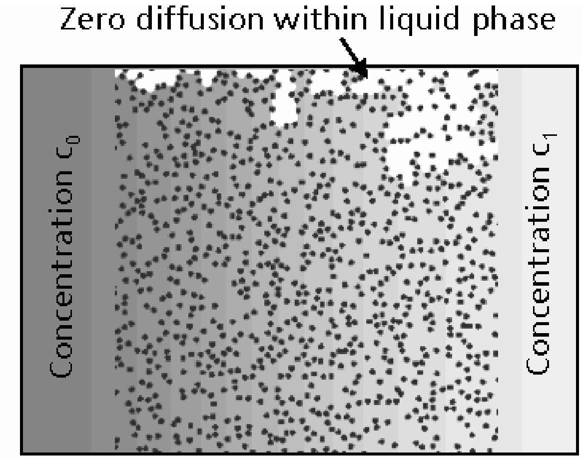

Fig. 5: Sketch of the setup for the calculation of the diffusion coefficient on a microscopic level in a 2D sample. The pore space of the hydrophobic media is partly water saturated derived from the simulated drainage process.

5 Simulation results

5.1 Absolute parameters

For the simulated carbon paper we calculated the absolute values, i.e. at 100% gas saturation, of the permeability, the effective gas diffusion, and the effective heat transfer coefficient. The following Table shows the results for in-plane and through-plane directions.

	In-plane	Through-plane
Permeability (Through-plane)	11.5 darcy	6.2 darcy
Effective gas diffusion (Through-plane) Tortuosity	0.62 1.14	0.56 1.20
Effective heat transfer	0.0092	0.0014

The Lattice Boltzmann simulation of the Stokes flow in the 3D structure of the carbon paper leads to an absolute permeability of 6.2 Darcy which is in good agreement with the measured value of 8 Darcy [1].

5.2 Relative parameters

5.2.1 Capillary pressure-saturation relation

The resulting capillary pressure-saturation curve of the investigated carbon paper is shown in Fig. 6

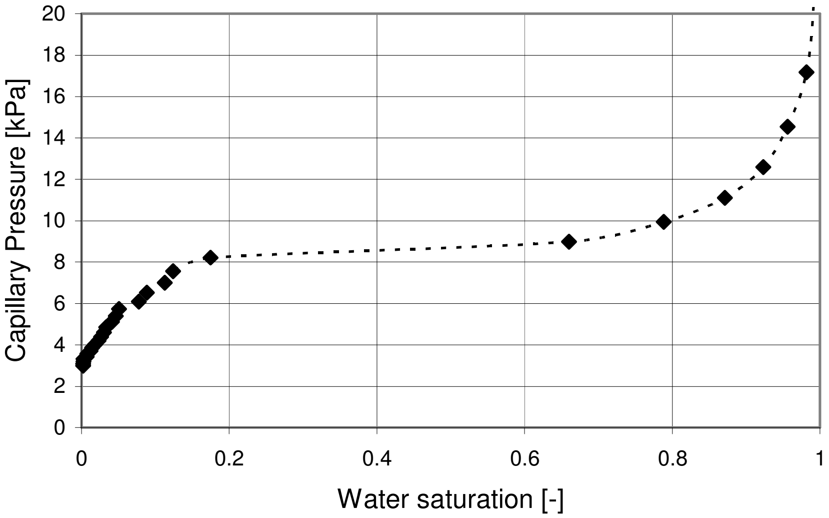

Fig. 6: Capillary pressure-saturation curve as a result of the simulated drainage process.

As one can see from Fig. 6, in the simulation the saturation changes significantly at a capillary pressure between 8 and 9 kPa. That pressure corresponds to the bubble point of the material. The bubble point is defined as the pressure where the water for the first time creates a full path between the two opposite sides of the sample. This is illustrated in Fig. 2 on the right hand side.
Following [1] our simulation results overestimate the measured bubble point by a factor of about 2. Nevertheless, this is result is promising since we based the reconstruction of the carbon paper on very view material parameters only.

5.2.2 Relative permeability and relative gas diffusion

The relative permeability and the relative gas diffusion coefficients in in-plane direction are given in the Fig. 7 and 8. The simulation results show the strong non-linear dependency on the water saturation. A comparison to measured data based on more information on the 3D geometry will be carried out in the near future.

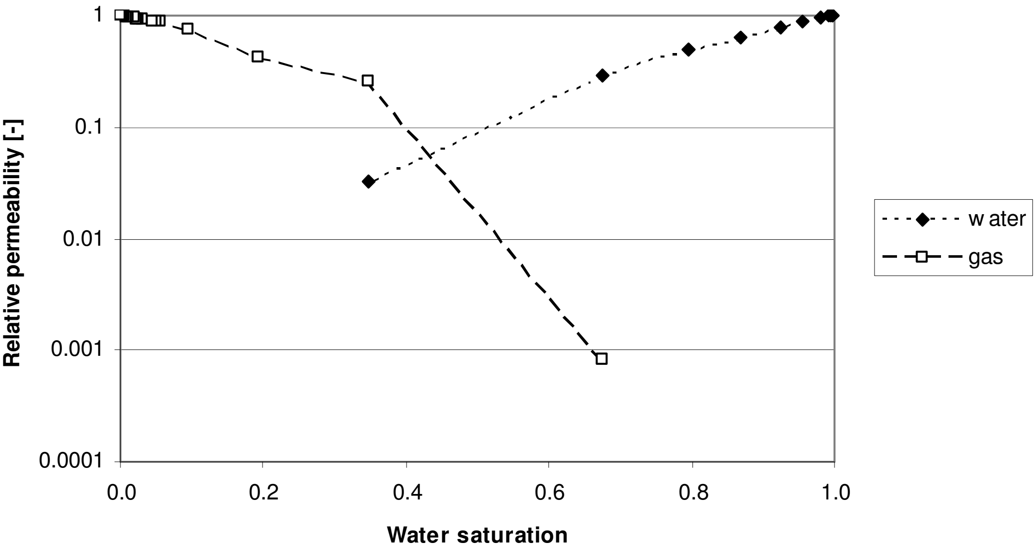

Fig. 7: Results for the simulated relative permeability of each phase as a function of the water saturation.

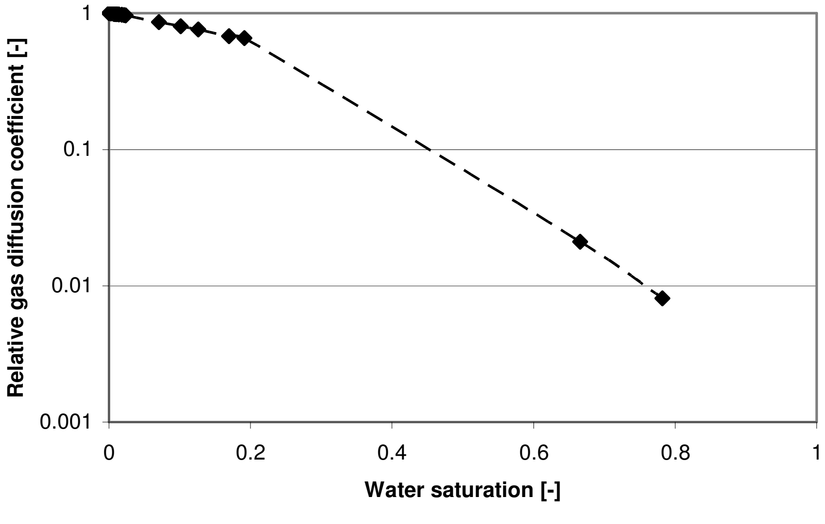

Fig. 8: Relative gas diffusion coefficient as a function of the water saturation. At the bubble point at a saturation between 0.2 and 0.6 the gas diffusion is reduced by two orders of magnitude.

6 Conclusion

In this paper we have shown a new approach for the determination of relative material parameters based on the underlying 3D microgeometry. Our method starts with an appropriate microstructure coming either from image giving methods techniques or by a virtual material design. Then, the phase distribution depending on the capillary pressure is determined by a full-morphology model where a primary drainage of the geometry is simulated. Based on the 3D phase distribution, we then calculate the relative material parameters under the assumption that we can decouple the physical process and the configuration of the phases. As a result, we get the permeability, the gas diffusion, and the heat conductivity of the material as a function of the saturation of media. The new approach had been applied to a virtually designed carbon paper used as a diffusion media in fuel cell. The simulation results show the expected trend in saturation dependent material parameters while more elaborated studies in comparison to measured data will follow in the near future.

7 Acknowledgements

Part of the author's research was funded by the Deutsche Forschungsgemeinschaft (German Research Council) via the project “Kombination von Lattice-Boltzmann- und Level-Set-Methoden für Fluid-Struktur-Interaktionen und Mehrphasenströmungen (STE 871/1-1)”.

Parts of the work took also benefit from the EU-CRAFT Project „Design of Innovative Non-wovens to be used as Insole in functional Shoes“.

8 References

[1] Eppstein, N.: “On tortuosity and tortuosity factor in flow and diffusion in porous media”, Chemical Engineering Science, Vol. 44/3, 1989, 777-779

[2] Hilpert, M., Miller, C.T. :”Pore-morephology-based simulation of drainage in totally wetting porous media”, Advances in Water Resources, 2001, pp. 243-255

[3] Kehrwald, D.:”Parallel lattice Boltzmann simulation of complex flows”, Tagungsband des ersten NAFEMS-CFD-Simunars, Niedernhausen b. Wiesbaden, Mai 2004

[4] Kehrwald, D.:”Numerical Anlaysis of Immiscible Lattice BGK”, Ph.D.-thesis, Universität Kaiserslautern, 2002

[5] Mathias, M., Roth, J., Fleming, J., and Lehnert, W.: “Diffusion media materials and characterization”, in: Handbook of Fuel Cells – Fundamentals, Technolgy and Applications”, Chapter 46, 2003, pp. 1-21

[6] McNamarea, G.R., Zanetti, G.: ”Use of the Boltzmann equation to simulate lattice gas automata”, Phys. Rev. Lett. 61, 1988, pp. 2332-2335

[7] Schladitz, K., Peters, S., Reinel-Bitzer, D., Wiegmann, A., and Ohser, J.: “Design of acoustic trim based on geometric modeling and flow simulation for non-woven”, Bericht des Fraunhofer ITWM, Nr. 72, 2005

[8] Schulz, V., Andrä, H.: “Acoustic trim optimization”, in: Proceedings of the Joint Congress CFA/DAGA’04, Strasbourg, March 22-25, 2004, Volume I, pp. 1-2

[9] Schulz, V. :”Description and reconstruction of microscopic random heterogeneous media in order to estimate macroscopic hydraulic functions”, Ph.D. thesis, Universität Heidelberg, 2003

[10] Soille, P.: “Morphological image anlaysis: principles and applications”, Springer Verlag Heidelberg, 1999

[11] Vogel, H.-J., Tölke, J., Schulz, V. P., Krafczyk, M., Roth, K.: “Comparison of a Lattice-Boltzmann model, a full-morphology model, and a pore network model for determining capillary pressure-saturation relationships”, accepted for publication in Vadose Zone Journal.

[12] Wiegmann, A., Zemitis, A.: “A fast iterative solver for the three-dimaensional virtual material design of the diffusivity of porous materials”, in prep.